文章编号 1004-924X(2016)01-0195-08

基于灰度线性建模的亚像素图像抖动量计算

智喜洋[1],侯晴宇[1*],王少游[2]
(1.哈尔滨工业大学 空间光学工程研究中心,黑龙江 哈尔滨 150001;
2.上海卫星工程研究所,上海 200240)

摘要:
。 , , 。 ,
, ,
, 。 ,
。 , 0.1 pixel。 ,
, 、 。

关 键 词:遥感图像;云场景;图像抖动量;亚像素;灰度线性建模
中图分类号:TP391;TP751 **文献标识码:**A **doi:**10.3788/OPE.20162401.0195

Estimation of image sub-pixel jitter based on linear model of image gray level

ZHI Xi-yang[1], HOU Qing-yu[1*], WANG Shao-You[2]

(1. *Research Center for Space Optical Engineering, Harbin Institute of Technology, Harbin* 150001, *China*;
2. *Shanghai Institute of Satellite Engineering, Shanghai* 200240, *China*)
* *Corresponding author, E-mail: houqingyu@126.com*

Abstract: A new method based on the linear model of image gray level was proposed to estimate sub-pixel jitters of a sequence image for cloud scene acquired by staring remote sensing imaging systems. Firstly, the image pixel and corresponding neighborhood gray levels were mathematically described by using linear model with three parameters, and the image gray was modeled. Then, by taking the jitter parameter as optimization variables in the linear mathematic model and the comparability between image sequences and reference frame as optimization objective, a new estimation method for the sub-pixel jitter was proposed based on least square optimization approach. Subsequently, the solving equation was derived. Finally, the method was verified by using simulated image sequences containing the cloud scene. Experimental results indicate that the proposed method is able to implement the subpixel estimation effectively and offers the estimation accuracy no less than 0.1 pixel. The obtained

收稿日期:2015-08-18;**修订日期:**2015-10-12.
基金项目:

estimation accuracy is higher than that of the conventional feature-based ones, and can be used in geometric calibration and target positioning of remote sensing images as well the multi-frame relative detection of time-series images.

Key words: remote sensing image; cloud scene; image jitter estimation; sub-pixel; model of image gray level

1 引 言

[1-2]

[3-5],

[6-9]

[10-16]。

[17],

[18-20]。

2 图像灰度线性建模

$\boldsymbol{B}_0$, (i,j)

:

$$\hat{\boldsymbol{B}}_0(i+k,j+m)=a_{ij}+g_{ij}\cdot m+h_{ij}\cdot k, \quad (1)$$

:$(k,m)\in\{(0,0),(0,-1),(0,1),(-1,0),(1,0)\}$,$(a_{ij},g_{ij},h_i$

$$\frac{\partial f}{\partial g_{ij}} = \sum_{k,m} 2 \cdot [\mathbf{B}_0(i+k, j+m) - (a_{ij} + g_{ij} m + h_{ij} k)] \cdot (-m) = 0,$$

$$\frac{\partial f}{\partial h_{ij}} = \sum_{k,m} 2 \cdot [\mathbf{B}_0(i+k, j+m) - (a_{ij} + g_{ij} m + h_{ij} k)] \cdot (-k) = 0. \tag{4}$$

：

$$\begin{pmatrix} \sum_{k,m} \mathbf{B}_0(i+k, j+m) \\ \sum_{k,m} m \cdot \mathbf{B}_0(i+k, j+m) \\ \sum_{k,m} k \cdot \mathbf{B}_0(i+k, j+m) \end{pmatrix} = \begin{pmatrix} \sum_{k,m} 1 & \sum_{k,m} m & \sum_{k,m} k \\ \sum_{k,m} m & \sum_{k,m} m^2 & \sum_{k,m} k \cdot m \\ \sum_{k,m} k & \sum_{k,m} k \cdot m & \sum_{k,m} k^2 \end{pmatrix} \begin{pmatrix} a_{ij} \\ g_{ij} \\ h_{ij} \end{pmatrix} = \mathbf{A} \cdot \quad a_i$$

，δ_x^n，δ_y^n
（11） 。
，
，，
。
，
，。

4 仿真验证

4.1 仿真验证方法

，
，
。
，3
（ 1 ）；
（ 29 ） （ 、 、 、
）、 1～3 pixel（ ）
，，；
，
3 ，；
，（ ），

，，
（RMSE），
。

4.2 灰度线性建模结果

1 ， 2
，3
（54，51） （70，78）
。

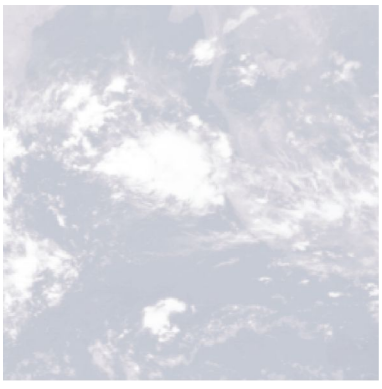

1
Fig. 1 Original high resolution remote sensing image of cloud scene

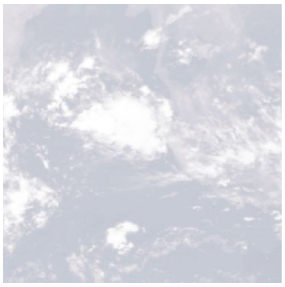

（a） 1 （ ）
(a) The 1st frame (reference)

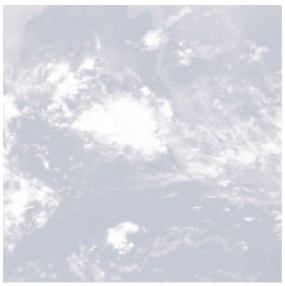

（b） 6
(b) The 6th frame

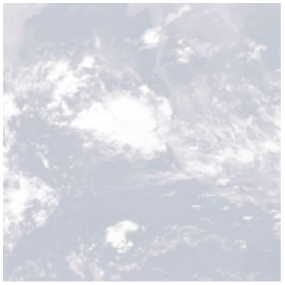

（c） 11
(c) The 11st frame

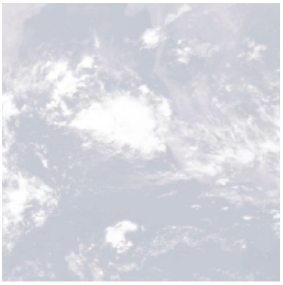

（d） 16
(d) The 16th frame

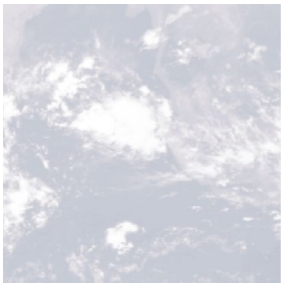

（e） 24
(e) The 24st frame

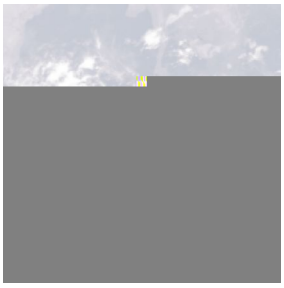

（f） 30
(f) The 30th frame

2
Fig. 2 Simulated low resolution images with jitter

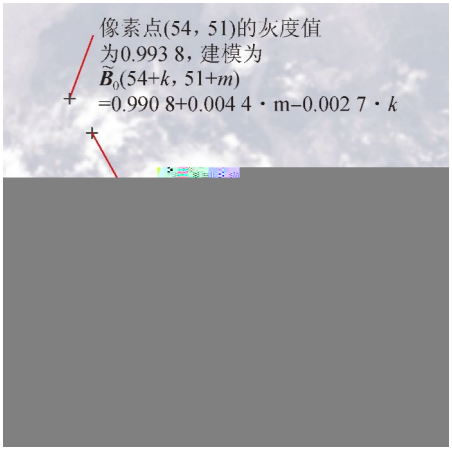

3
Fig. 3 Modelling results of reference frame

4.3 抖动量计算结果

4(a) (b)、(e) (f)、(i) (j)

x 、y ，
4(c) (d)、(g) (h)、(k) (l)
。 ， “×”
，“Δ” 。
，
， 10^{-1} ，
10^{-3} 。

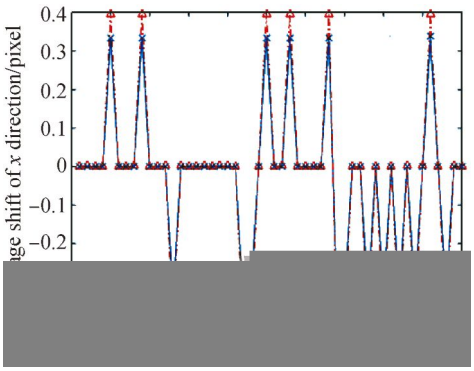

(a) 1 x

(a) Result in x direction with amplitude of 1 pixel

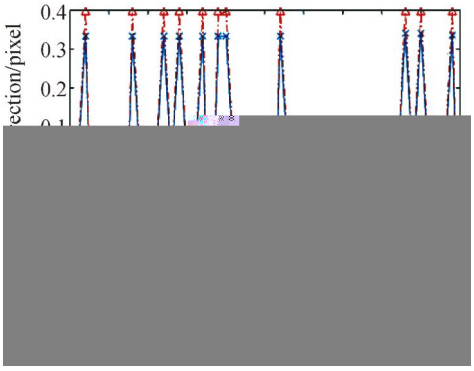

(b) 1 y

(b) Result in y direction with amplitude of 1 pixel

(c) (a) x

(c) RMSE of (a) in x direction

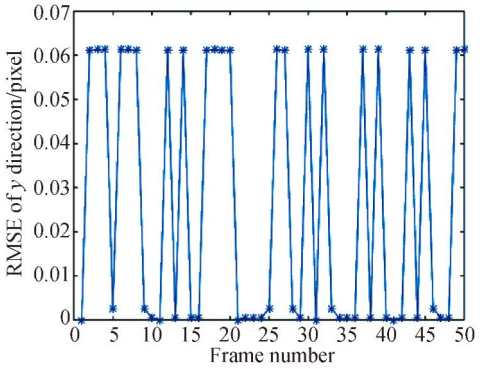

(d) (b) y

(d) RMSE of (b) in y direction

(e) 2 x

(e) Result in x direction with amplitude of 2 pixel

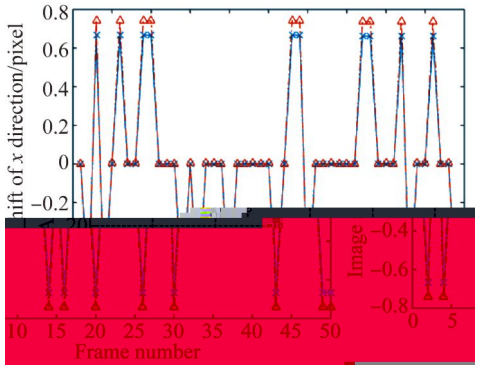

(f) 2 y

(f) Result in y direction with amplitude of 2 pixel

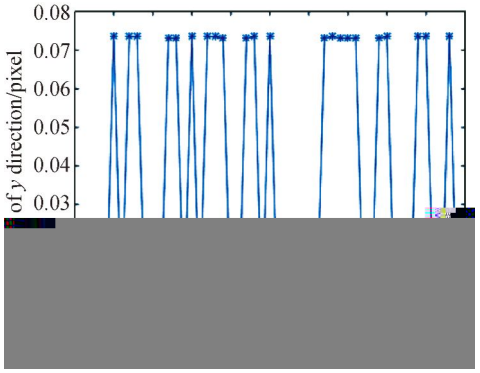

(g) (e) x

(g) RMSE of (e) in x direction

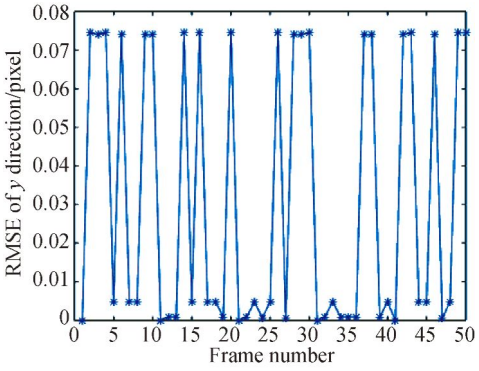

(h) (f) y

(h) RMSE of (f) in y direction

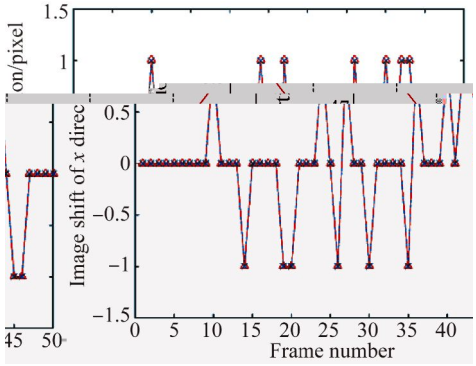

(i) 3 x

(i) Result in x direction with amplitude of 3 pixel

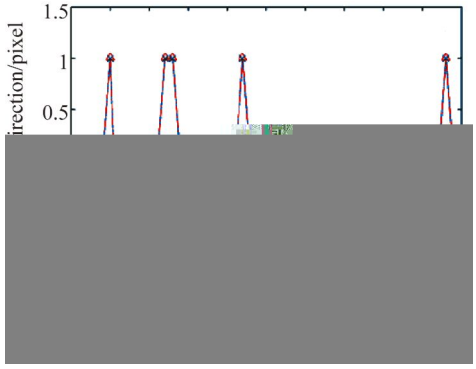

(j) 3 y

(j) Result in y direction with amplitude of 3 pixel

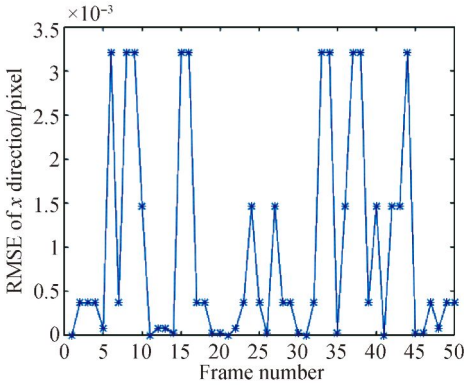

(k) (i) x

(k) RMSE of (i) in x direction

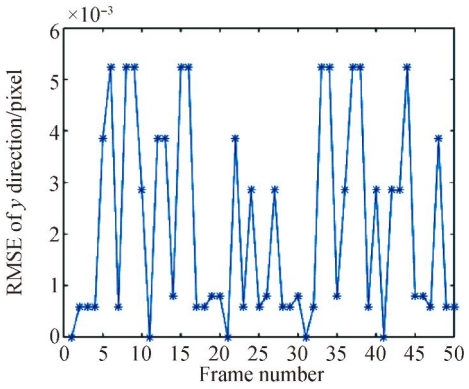

(l) (j) y

(l) RMSE of (j) in y direction

4

Fig. 4 Results and corresponding errors of jitter estimation for image sequences

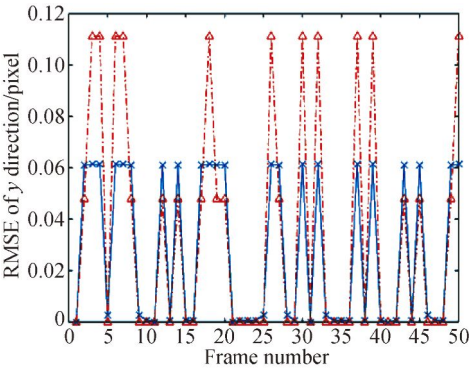

5 1 y

Fig. 5 Comparison of RMSE between proposed algorithm and conventional ones in y direction with amplitude of 1 pixel

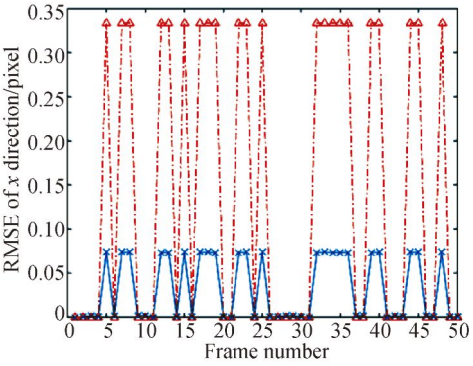

6 2 x

Fig. 6 Comparison of RMSE between proposed algorithm and conventional ones in x direction with amplitude of 2 pixel

, [21]

。 [21]

(SIFT) ,

,

。

, 。
, ,
, 。 5、 6 ,
1 y 2 。 ,
x , ,
, 。 ,
。

5 结 论

, 、
,
,
。

参考文献:

[1] PARIS C. Vibration tests on the preloaded LARES satellite and separation system [J]. *Aerospace Science and Technology*, 2015, 42: 470-476.

[2] ZHI X Y, HOU Q Y, SUN X, *et al.*. Degradation and restoration of high resolution TDICCD imagery due to satellite vibrations [C]. *International Symposium on Optoelectronic Technology and Application 2014, International Society for Optics and Photonics*, 2014: 93012I-1-93012I-8.

[3] LIN CH, LIN B Y, LEE K Y, *et al.*. Radiometric normalization and cloud detection of optical satellite images using invariant pixels [J]. *ISPRS Journal of Photogrammetry and Remote Sensing*, 2015, 106: 107-117.

[4] ZHU Z, WANG S X, WOODCOCK C E. Improvement and expansion of the Fmask algorithm: cloud, cloud shadow, and snow detection for Landsats 4-7, 8, and Sentinel 2 images [J]. *Remote Sensing of Environment*, 2015, 159: 269-277.

[5] JAYADEVAN V T, RODRIGUEZ J J, CRONIN A D. A new contrast-enhancing feature for cloud detection in ground-based sky images [J]. *Journal of Atmospheric and Oceanic Technology*, 2015, 32 (2): 209-219.

[6] 聂宏宾, 侯晴宇, 赵明, 等. EM [J]. 光学 精密工程, 2011, 19(3): 657-663.
NIE H B, HOU Q Y, ZHAO M, *et al.*. IR/visible image registration based on EM iteration of log-likelihood function [J]. *Opt. Precision Eng.*, 2011, 19(3):658-663. (in Chinese)

[7] WU T J, GE Y, WANG J, *et al.*. A WTLS-based method for remote sensing imagery registration [J]. *IEEE Transactions on Geoscience and Remote Sensing*, 2015, 53(1): 102-116.

[8] WU Y, MA W, GONG M, *et al.*. A novel point-matching algorithm based on fast sample consensus for image registration [J]. *Geoscience and Remote Sensing Letters, IEEE*, 2015, 12(1): 43-47.

[9] 林培杰, 郑柏春, 陈志聪, 等. [J]. 液晶与显示, 2015, 30 (3):484-491.
LIN P J, ZHENG B CH, CHEN ZH C, *et al.*. System of multi-regions moving object detection in video surveillance [J]. *Chinese Journal of Liquid Crystals and Displays*, 2015, 30(3):484-491. (in Chinese)

[10] KUPFER B, NETANYAHU N S, SHIMSHONI I. An efficient SIFT-based mode-seeking algorithm for sub-pixel registration of remotely sensed images [J]. *Geoscience and Remote Sensing Letters, IEEE*, 2015, 12(2): 379-383.

[11] JIANG J, ZHANG S, CAO S. Rotation and scale invariant shape context registration for remote sensing images with background variations [J]. *Journal of Applied Remote Sensing*, 2015, 9(1): 095092-1-095092-20.

[12] TENG S W, HOSSAIN M T, LU G. Multimodal image registration technique based on improved local feature descriptors [J]. *Journal of Electronic Imaging*, 2015, 24(1): 013013-1-013013-17.

[13] WANG Z, KIEU H, NGUYEN H, *et al.*. Digital image correlation in experimental mechanics and image registration in computer vision: Similarities, differences and complements [J]. *Optics and Lasers in Engineering*, 2015, 65: 18-27.

[14] 王洪涛, 李丹.

[J]. 液晶与显示, 2014, 29(5):800-804.
WANG H T, LI D. Image edge detection research based on improved particle swarm optimization algorithm [J]. *Chinese Journal of Liquid Crystals and Displays*, 2014, 29(5):800-804. (in Chinese)

[15] 李志军, 刘松林, 牛照东,等.
Hausdorff [J]. 红外与激光工程, 2015, 44(2):775-780.
LI ZH J, LIU S L, NIU ZH D, *et al.*. Hausdorff distance template matching method based on gradient phase and significance constraints [J]. *Infrared and Laser Engineering*, 2015, 44(2): 775-780. (in Chinese)

[16] 赵爱罡, 王宏力, 杨小冈,等.
SIFT [J]. 红外与激光工程, 2015, 44(3):1085-1091.
ZHAO A G, WANG H L, YANG X G, *et al.*. Compressed sense SIFT descriptor mixed with geometrical feature [J]. *Infrared and Laser Engineering*, 2015, 44(3):1085-1091. (in Chinese)

[17] GHAFURIAN S, HACIHALILOGLUB I, METAXAS D N, *et al.*. 3D/2D image registration using weighted histogram of gradient directions [C]. *SPIE Medical Imaging*, *International Society for Optics and Photonics*, 2015: 94151Z-1-94151Z-7.

[18] AGANJ I, REUTER M, SABUNCU M R, *et al.*. Avoiding symmetry-breaking spatial non-uniformity in deformable image registration via a quasi-volume-preserving constraint [J]. *NeuroImage*, 2015, 106: 238-251.

[19] DURAISAMY P, YOUSEF A, BUCKLES B, *et al.*. Image registration under symmetric conditions: novel approach [C]. *Proc. SPIE* 9477, *Optical Pattern Recognition XXVI*, 94770N, 2015: 1-5.

[20] LEE I H, MAHMOOD M T. Robust registration of cloudy satellite images using two-step segmentation[J]. *Geoscience and Remote Sensing Letters, IEEE*, 2015, 12(5): 1121-1125.

[21] LOWE D G. Distinctive image features from scale-invariant keypoints [J]. *International Journal of Computer Vision*, 2004, 60(2): 91-110.

作者简介:

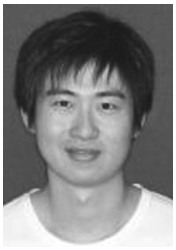

智喜洋(1982—), , , ,2012
, 、
。E-mail:zhixiyang@hit.edu.cn

通讯作者:

侯晴宇(1982—), , , ,2011
, 、
。E-mail:houqingyu@126.com